Preprints of the 21st IFAC World Congress (Virtual)
Berlin, Germany, July 12-17, 2020

Global Sensitivity Analysis on the Torque Accuracy of the Powertrain in Electric Vehicles

Matthias Braband * **Michael Adams** * **Andreas Wilhelmi** **
Matthias Scherer *

* *University of Applied Sciences Trier, Institute of Energy Efficient Systems, Schneidershof, D-54293 Trier (corresponding e-mail: M.Braband@hochschule-trier.de)*
** *hofer eds GmbH, Sedanstraße 21b, 97082 Würzburg (e-mail: Andreas.Wilhelmi@hofer.de)*

Abstract: Electric drive systems are increasingly used in automobiles. However, the combination of comfort, dynamics and safety requirements places high demands on the torque accuracy. The complex interplay of battery, inverter and electrical machine causes a lot of system uncertainties based on parameter fluctuations and measurement errors that influence the system performance. In this paper these influences on the closed loop torque control are analyzed and quantified using a variance based sensitivity analysis. The method enables to connect the variance of the torque accuracy with the parameter uncertainties causing this variance. Moreover, it quantifies the influences of the parameters independent of the complexity of the analyzed system. In addition, two methods to ensure convergence of the estimated variance based sensitivity measures are proposed. The results of the analysis are presented for 19 static working points of an battery electric drive system.

Keywords: Sensitivity analysis, electrical drive, BEV, electromobility, control systems, Monte Carlo simulation

1. INTRODUCTION

Electric drives are increasingly used in the powertrain of automobiles. Due to high safety demands the requirements on the torque accuracy of the electric drive system are considerably high. Because the direct measurement of the torque is to elaborate, it is indirectly calculated based on the measured phase currents of the drive. However, this calculation includes temperature and working point dependent parameters such as the inductances and the magnetic flux. Also, the drive system underlies manufacturing tolerances in the series production. In addition, the measurements of the mechanical angle, the phase currents and of the DC-link voltage are influenced by measurement errors. They directly affect the accuracy of the requested torque.

In practice, it would be time and cost consuming to calibrate each powertrain to both its varying parameters and its measurement errors. Therefore, the control system needs to be robust against parameter and measurement fluctuations. To still increase the robustness and the torque accuracy the question arises which parameter has which amount of influence on the torque deviation.

However, it is not possible to quantify the influences of parameter fluctuations in such a complex technical system with established control theory methods. Therefore, this paper presents a variance based sensitivity approach, introduced by Sobol (1993), to quantify the relation between the variance of the output of interest and its causes. This method is already used in several technical applications, for example Schwieger (2007), Menberg et al. (2016) and Opalski (2015). These authors stated that it is a powerful tool to analyze technical systems or models. In this paper the variance based analysis identifies the most influencable parameters in order to improve the torque accuracy of the drive system.

The variance based sensitivity indices cannot be calculated analytically. Instead of they are estimated based on pseudo Monte Carlo simulations. This raises the problem of ensuring convergence of the estimators which is to the best of our knowledge neglected in the literature. Therefore, this paper presents a novel approach to ensure convergence of the estimated sensitivity indices.

The theory on sensitivity analysis and convergence is presented in Section 2. The sensitivity measures are computed for a real drive system of a battery electric vehicle (BEV). The used model is described in Section 3. The corresponding sensitivity setup is explained in Section 4. The results of the sensitivity analysis and also the convergence of the estimators are presented and discussed in Section 5. Section 6 summarizes the results and draws conclusions.

2. VARIANCE BASED SENSITIVITY ANALYSIS

Considering the relation between the output Y and the input X can be described by the model $Y = f(X_1, X_2, \ldots, X_K)$ with K parameters. In the variance based sensitivity analysis the variation of each input pa-

rameter X_i is specified by their probability density functions (PDF). The model can be decomposed using a high dimensional model representation (HDMR), first introduced by Sobol (1993), into

$$y = f(\mathbf{x}) = f_0 + \sum_{i=1}^{K} f_i(x_i) + \sum_{i=1}^{K}\sum_{i<j}^{K} f_{ij}(x_i, x_j) + \ldots + f_{12\ldots K}(x_1, x_2, \ldots, x_K), \tag{1}$$

where f_0 denotes a constant. The term $\sum_{i=1}^{K} f_i(x_i)$ includes a set of K functions depending on a single parameter x_i. The term $\sum_{i=1}^{K}\sum_{i<j}^{K} f_{ij}(x_i, x_j)$ describes a set of functions including interaction terms between two parameters x_i, x_j. This scheme of decomposition can be continued to $f_{12\ldots K}(x_1, x_2, \ldots, x_K)$ which describes the interaction between the complete parameter set K.

Assuming independence between the parameters the variance of Equation (1) is given by

$$V(Y) = \sum_{i=1}^{K} V_i + \sum_{i=1}^{K}\sum_{i<j}^{K} V_{ij} + \ldots + V_{12\ldots K}. \tag{2}$$

Normalizing Equation (2) by $V(Y)$ leads to

$$1 = \sum_{i=1}^{K} S_i + \sum_{i=1}^{K}\sum_{i<j}^{K} S_{ij} + \ldots + S_{12\ldots K}, \tag{3}$$

which represents a decomposition of the sources of variance. S_i denotes the first order effect. It quantifies the influence of a single parameter on the output of interest. S_{ij} are called second order effects and indicate the interaction between two parameters. This scheme can be continued up to the effects of K-th order.

To describe all effects of one parameter the total effect

$$S_{T_i} = S_i + \sum_{\substack{j=1 \\ j\neq i}}^{K} S_{ij} + \ldots + S_{12\ldots K} \tag{4}$$

sums up all effects including its interaction effects on the output of interest.

The decomposition in Equation (3) leads to $2^K - 1$ possible sensitivity measures. Due to this large amount of indices it is impractical to analyze all effects. Furthermore, the first order and total order effects represent a satisfactory approximation of the overall system behavior. Therefore, in this paper only the first order and total effects are used.

As shown in Saltelli et al. (2010), the first order indices can be calculated by the relation of the conditional expectation value $V_{X_i}(E_{\mathbf{X}_{\sim i}}(Y \mid X_i))$ and the overall variance $V(Y)$ described by

$$S_i = \frac{V_{X_i}(E_{\mathbf{X}_{\sim i}}(Y \mid X_i))}{V(Y)}. \tag{5}$$

$\mathbf{X}_{\sim i}$ denotes the vector of all parameters except X_i. The inner expectation operator outlines the averaging over all possible values of $\mathbf{X}_{\sim i}$ while keeping X_i fixed. The outer variance is taken over all X_i.

For calculating the total effect the Equation

$$S_{Ti} = \frac{E_{\mathbf{X}_{\sim i}}(V_{X_i}(Y \mid \mathbf{X}_{\sim i}))}{V(Y)} = 1 - \frac{V_{\mathbf{X}_{\sim i}}(E_{X_i}(Y \mid \mathbf{X}_{\sim i}))}{V(Y)} \tag{6}$$

holds. The question arises how to compute $V_{X_i}(E_{\mathbf{X}_{\sim i}}(Y \mid X_i))$ for the first order effects in Equation (5) and $E_{\mathbf{X}_{\sim i}}(V_{X_i}(Y \mid \mathbf{X}_{\sim i}))$ for the total effects in Equation (6). Using sample data it is not possible to calculate the sensitivity indices analytically. Therefore, $V_{X_i}(E_{\mathbf{X}_{\sim i}}(Y \mid X_i))$, $E_{\mathbf{X}_{\sim i}}(V_{X_i}(Y \mid \mathbf{X}_{\sim i}))$ and $V(Y)$ are replaced by their corresponding estimates $\hat{V}_{X_i}(E_{\mathbf{X}_{\sim i}}(Y \mid X_i))$, $\hat{E}_{\mathbf{X}_{\sim i}}(V_{X_i}(Y \mid \mathbf{X}_{\sim i}))$ and $\hat{V}(Y)$.

2.1 Estimation of first order and total order effects

For the sample data generation quasi-random sequences are used. Sobol and Kucherenko (2005) showed that quasi-random sequences converge faster than crude Monte Carlo sampling (random sampling). This applies in particular for sequences with low discrepancy values. Therefore, in this paper, Sobol sequences (Sobol, 1967) are used as the most common representative of quasi-random sequences.

The sample data are generated in the unit hypercube with two independent sampling matrices using Sobol sequences. The distribution of each parameter can be transformed from the uniform distribution in the unit hypercube to any other cumulative distribution function (CDF) using its inverse. This results in the sampling matrices, as proposed in Saltelli et al. (2010),

$$\mathbf{A} = \begin{bmatrix} a_{11} & a_{12} & \cdots & a_{1K} \\ a_{21} & \ddots & & \vdots \\ \vdots & & \ddots & \vdots \\ a_{N1} & \cdots & \cdots & a_{NK} \end{bmatrix} \quad \text{with} \quad a_{jg} \in \mathbb{R}^{N\times K} \tag{7}$$

$$\mathbf{B} = \begin{bmatrix} b_{11} & b_{12} & \cdots & b_{1K} \\ b_{21} & \ddots & & \vdots \\ \vdots & & \ddots & \vdots \\ b_{N1} & \cdots & \cdots & b_{NK} \end{bmatrix} \quad \text{with} \quad b_{jg} \in \mathbb{R}^{N\times K} \tag{8}$$

where the index $g \in \{1, 2, ..., K\}$ denotes the parameter of interest and the index $j \in \{1, 2, ..., N\}$ denotes the number of simulation.

For the estimators a third dataset

$$\mathbf{A}_{\mathbf{B}}^{(i)} = \begin{bmatrix} a_{11} & \cdots & b_{1i} & \cdots & a_{1K} \\ a_{21} & & b_{2i} & & \vdots \\ \vdots & & \vdots & & \vdots \\ a_{N1} & \cdots & b_{Ni} & \cdots & a_{NK} \end{bmatrix} \tag{9}$$

is obtained from matrix $\mathbf{A}$ where the i-th column is replaced by the i-th column from matrix $\mathbf{B}$. With the sampling matrices $\mathbf{A}$ and $\mathbf{A}_{\mathbf{B}}^{(i)}$ S_i and S_{T_i} can be estimated with different estimators. In this paper, three estimators for the first order effects, introduced by Sobol (1993), Jansen (1999) and Saltelli et al. (2010), are compared. For the total effects two estimators, suggested by Jansen (1999) and Sobol (2007), are analyzed. All estimators under consideration are summarized in Table (1).

For the estimation of the denominators of Equations (5) and (6) the sample variance

$$\hat{V}(Y) = \frac{1}{N-1}\sum_{i=1}^{N}(Y - \overline{Y})^2 \tag{10}$$

is used.

Table 1. First order and total order estimators

$\hat{V}_{X_i}(E_{\mathbf{X}_{\sim i}}(Y \mid X_i))$	Author
$\frac{1}{N}\sum_{j=1}^{N} f(\mathbf{A})_j f(\mathbf{B}_{\mathbf{A}}^{(i)})_j - f_0^2$	Sobol (1993)
$V(Y) - \frac{1}{2N}\sum_{j=1}^{N}\left(f(\mathbf{B})_j - f(\mathbf{A}_{\mathbf{B}}^{(i)})_j\right)^2$	Jansen (1999)
$\frac{1}{N}\sum_{j=1}^{N} f(\mathbf{B})_j\left(f(\mathbf{A}_{\mathbf{B}}^{(i)})_j - f(\mathbf{A})_j\right)$	Saltelli et al. (2010)
$\hat{E}_{\mathbf{X}_{\sim i}}(V_{X_i}(Y \mid \mathbf{X}_{\sim i}))$	
$\frac{1}{2N}\sum_{j=1}^{N}\left(f(\mathbf{A})_j - f(\mathbf{A}_{\mathbf{B}}^{(i)})_j\right)^2$	Jansen (1999)
$\frac{1}{N}\sum_{j=1}^{N} f(\mathbf{A})_j\left(f(\mathbf{A}) - f(\mathbf{A}_{\mathbf{B}}^{(i)})_j\right)$	Sobol (2007)

The performance of these estimators, also for non normal distributed input parameters, is outlined in Saltelli et al. (2010) for different test cases.

2.2 Time and state dependence of physical systems

The major drawback of the HDMR, as defined in Equation (1), is that time and state dependencies are neglected. Considering time and state dependencies the model can be described by

$$y(t) = f(\mathbf{x}_p, \mathbf{x}_0, t, \mathbf{u}(t)), \tag{11}$$

where $\mathbf{x}_p$ denotes the parameters of interest. The vector $\mathbf{x}_0$ is the initial system state and t represents the point in time of the physical system. Common physical system are equipped with a control input $\mathbf{u}(t)$. The extension of the system by x_0, t and $\mathbf{u}(t)$ leads to state and time dependent sensitivity indices expressed by

$$S_i(\mathbf{x}_0, t, \mathbf{u}(t)) \tag{12}$$
$$S_{T_i}(\mathbf{x}_0, t, \mathbf{u}(t)). \tag{13}$$

In order to guarantee representative sensitivity results the whole state space of the system has to be covered.

2.3 Convergence behavior

For reliable sensitivity estimates it is essential to ensure convergence of the estimators. Also it needs to be ensured that the available data, defined by the number of samples N, is large enough for producing reliable estimates. In the following, two approaches to verify convergence are discussed.

The first method calculates an absolute scalar error measure over all estimates, whereas the second method approximates the confidence intervals for each estimated value $\hat{S}_i(\mathbf{x}_0, t, \mathbf{u}(t))$ and $\hat{S}_{T_i}(\mathbf{x}_0, t, \mathbf{u}(t))$.

The former method is based on the fact that each estimator in Table (1) ensures asymptotic unbiased results which means that

$$\lim_{N\to\infty} \hat{S}_i(\mathbf{x}_0, t, \mathbf{u}(t)) = S_i(\mathbf{x}_0, t, \mathbf{u}(t)) \tag{14}$$
$$\lim_{N\to\infty} \hat{S}_{T_i}(\mathbf{x}_0, t, \mathbf{u}(t)) = S_{T_i}(\mathbf{x}_0, t, \mathbf{u}(t)). \tag{15}$$

In the first step the parameters $\mathbf{x}_0, t$ and $\mathbf{u}(t)$ need to be removed from Equations (11), (12) and (13). $\mathbf{x}_0$ and $\mathbf{u}(t)$ have to be selected such that all working points of interest are covered. This choice highly depends on the analyzed physical system. The remaining time dependency

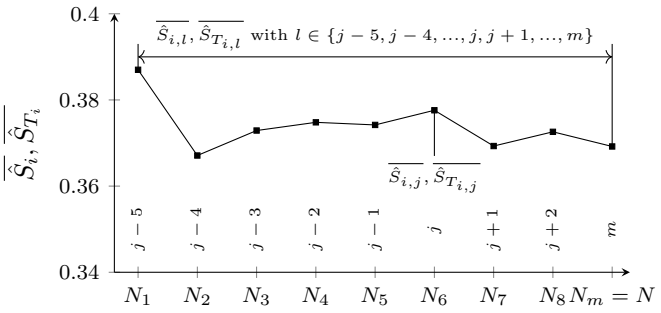

Fig. 1. Exemplary estimation result for $\overline{\hat{S}_i}, \overline{\hat{S}_{T_i}}$ with different sample sizes $[N_1, N_m]$ for parameter i

is removed by computing the mean over the time interval $[t_1, t_2]$ with

$$\overline{\hat{S}_i} = \frac{1}{t_2 - t_1}\int_{t_1}^{t_2} \hat{S}_i(t)\mathrm{d}t \tag{16}$$
$$\overline{\hat{S}_{T_i}} = \frac{1}{t_2 - t_1}\int_{t_1}^{t_2} \hat{S}_{T_i}(t)\mathrm{d}t. \tag{17}$$

Accordingly, (16) and (17) represent a scalar measure.

To verify the convergence of the estimators, so called error measures need to be determined. Initially, the sensitivity measures $\overline{\hat{S}_i}$ and $\overline{\hat{S}_{T_i}}$ are estimated for different sample sizes $N_1 < N_2 < ... < N_m = N$. Then the error measures are obtained from

$$\varepsilon_{\overline{\hat{S}_{i,j}}} = \max_l \left|\overline{\hat{S}_{i,j}} - \overline{\hat{S}_{i,l}}\right| \tag{18}$$
$$\varepsilon_{\overline{\hat{S}_{T_{i,j}}}} = \max_l \left|\overline{\hat{S}_{T_{i,j}}} - \overline{\hat{S}_{T_{i,l}}}\right| \tag{19}$$

with $j \in \{1, 2, ..., m\}$ and $l \in \{j-5, j-4, ..., j, j+1, ..., m\}$. For a better understanding of Equations (18) and (19) Figure 1 underlines the relations between the sample sizes and the different indices. Because of (14) and (15), it is obvious that the measures in Equations (18) and (19) tend to zero for increasing sample sizes.

To get a single measure of the complete estimation the mean over all parameters

$$\overline{\varepsilon_{\hat{S}_j}} = \frac{1}{K}\sum_{i=1}^{K} \overline{\varepsilon_{\hat{S}_{i,j}}} \tag{20}$$
$$\overline{\varepsilon_{\hat{S}_{T_j}}} = \frac{1}{K}\sum_{i=1}^{K} \overline{\varepsilon_{\hat{S}_{T_{i,j}}}} \tag{21}$$

is computed with K as the number of parameters.

Finally, convergence of the estimators is ensured if $\overline{\varepsilon_{\hat{S}_j}}, \overline{\varepsilon_{\hat{S}_{T_j}}} \leq \varepsilon_{max}$, where ε_{max} is a certain error bound.

The second method, which calculates the confidence interval for each estimated value $\hat{S}_i(\mathbf{x}_0, t, \mathbf{u}(t))$ and $\hat{S}_{T_i}(\mathbf{x}_0, t, \mathbf{u}(t))$, is based on bootstrap resampling introduced by Efron (1979). In bootstrap resampling the simulation results of sample size N are assumed to be the basic population. From this basic population a random sample of size $N_b < N$ is drawn randomly. This resampling is repeated B times. For each bootstrap sample, the sensitivity measures $\hat{S}_i^b$ and $\hat{S}_{T_i}^b$ are calculated. The estimated mean and standard deviation of these bootstrap samples

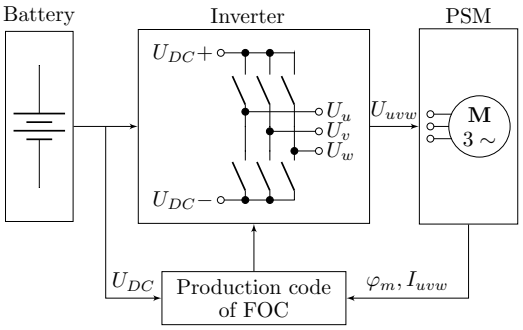

Fig. 2. System overview

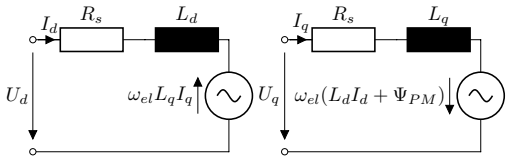

Fig. 3. PSM equivalent circuits

$$\overline{\hat{S}_i^b} = \frac{1}{B} \sum_{b=1}^{B} \hat{S}_i^b \tag{22}$$

$$\hat{\sigma}_{S_i^b} = \sqrt{\frac{1}{B-1} \sum_{b=1}^{B} (\hat{S}_i^b - \overline{\hat{S}_i^b})^2} \tag{23}$$

leads to the information for defining the confidence intervals. The estimated mean and standard deviation of the total effect $\hat{S}_{T_i}^b$ is analogously calculated to Equations (22) and (23). Archer et al. (1997) proved that the estimated mean and standard deviation using bootstrap resampling is asymptotically normal distributed and consistent formalized by

$$\lim_{B \to \infty} \overline{\hat{S}_i^b} = E(\hat{S}_i^b) = S_i^b \tag{24}$$

$$\lim_{B \to \infty} \hat{\sigma}_{S_i^b} = \sqrt{E((\hat{S}_i^b)^2) - E(\hat{S}_i^b)^2} = \sigma_{S_i^b}. \tag{25}$$

The definitions in Equations (24) and (25) are also valid when calculating the bootstrap samples for $\hat{S}_{T_i}^b$. The properties (24) and (25) enable the derivation of reliable confidence intervals, if the number of bootstrap samples B is large enough.

3. SIMULATION SETUP

The physical system under consideration is a common powertrain for an battery electric vehicle. Figure 2 illustrates that the physical system consists of a battery, an inverter and a permanent magnet synchronous drive (PSM). In addition, the real implemented production code software of the inverter is modeled. Because the focus of this analysis lies on investigating the effects of changing material parameters in the drive and measurement errors in the inverter, the battery is modeled as a constant voltage source. Also dynamic effects of the wiring are neglected in this simulation. The IGBTs of the inverter are modeled as ideal switches without any losses.

The PSM is designed as a fundamental wave model in d, q coordinates with saturation effects, as described in

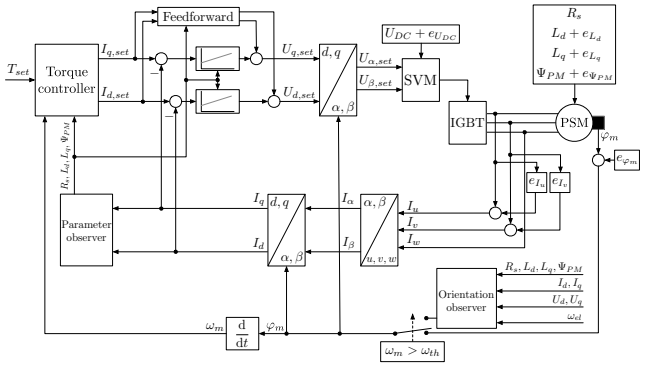

Fig. 4. Implemented field oriented control with error injection points

Schröder (2013). According to the equivalent circuit, as shown in Figure 3, the following voltage Equations results

$$U_d = R_s I_d + \frac{\mathrm{d}L_d(I_d, I_q) I_d}{\mathrm{d}t} - \omega_{el} L_q(I_d, I_q) I_q \tag{26}$$

$$U_q = R_s I_q + \frac{\mathrm{d}L_q(I_d, I_q) I_q}{\mathrm{d}t} + \omega_{el} L_d(I_d, I_q) I_d + \omega_{el} \Psi_{PM}(I_d, I_q). \tag{27}$$

The saturation effects are modeled by the dependence of the direct inductance L_d, the quadrature inductance L_q and the magnetic flux Ψ_{PM} on the currents I_d and I_q. The relationship between the controlled currents I_d and I_q and the air gap torque T_{el} is described by

$$T_{el} = \frac{3}{2} p I_q \Big(\Psi_{PM}(I_d, I_q) + I_d \big(L_d(I_d, I_q) - L_q(I_d, I_q) \big) \Big) \tag{28}$$

with p as the number of pole pairs.

The software model is the production code of a state of the art field-oriented control (FOC) of the hofer eds drive unit. Figure 4 displays the principle scheme.

4. SENSITIVITY SETUP

In the following, the influences of production related parameter variations on the PSM, caused by varying plate and magnet material, are examined. The variation of plate and magnet material results in a variation in the machine parameters L_d, L_q and Ψ_{PM}. Because the errors in the inductances and also the magnetic flux are working point dependent, as outlined in Figure 5, they are modeled as lookup tables. The maximum errors are previously defined by FEM simulations of the investigated machine. To model the working point dependence of L_d, L_q and Ψ_{PM} auxiliary variables $e_{L_d}, e_{L_q}, e_{\Psi_{PM}} \in [-1, 1]$ are introduced. By multiplying these auxiliary variables with the working point dependent lookup values, the maximum error in each working point is taken into account. In addition, the variation in the winding resistance R_s is also respected.

The measurement errors are considered for the current sensors e_{I_u}, e_{I_v}, the DC-link voltage sensor $e_{U_{DC}}$ and the mechanical angle sensor e_{φ_m}.

Figure 4 depicts the injection points of these errors. All parameter variations are assumed to be normal distributed.

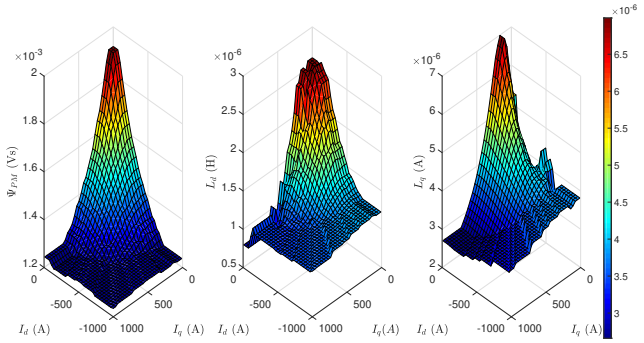

Fig. 5. Working point dependent error of the machine parameters L_d, L_q, Ψ_{PM}.

Table 2 summarizes their type of error and their variations.

Table 2. Parameter variations

Name	Type of error	Mean	Variance	3σ
R_s	absolute value	8.8 mΩ	7.744×10^{-6} mΩ^2	0.264 mΩ
e_{L_d}	percentage error	0	$\frac{1}{9}$	1
e_{L_q}	percentage error	0	$\frac{1}{9}$	1
$e_{\Psi_{PM}}$	percentage error	0	$\frac{1}{9}$	1
e_{I_u}	relative error	0	6.94×10^{-5}	0.025
e_{I_v}	relative error	0	6.94×10^{-5}	0.025
$e_{U_{DC}}$	relative error	0	1.11×10^{-5}	0.01
e_{φ_m}	absolute error	0 rad	2.11×10^{-6} rad^2	0.0044 rad

5. RESULTS

With the previously presented model and the sensitivity setup the Sobol sensitivity indices are calculated. Section 5.1 outlines the achieved convergence behavior of the analyzed system and section 5.2 discusses the simulation results.

5.1 Convergence behavior

In the following, the simulations results are examined with respect to the convergence behavior of the estimators. Figure 6 outlines the measures described in Equations (20) and (21). The estimators behave significantly different in their convergence behavior. The estimators from Jansen converges faster than the estimators from Sobol and Saltelli. For a maximum sample size of $N = 3000$ samples only the Jansen estimators reach the predefined error bound $\varepsilon_{max} = 0.01$.

The same convergence behavior can be observed in Figure 7, which presents the confidence intervals for $\hat{S}_i$ and $\hat{S}_{T_i}$ for a specific time interval using Bootstrap resampling. Comparing the Jansen estimators with the Sobol estimators, it becomes obvious that the 95% confidence error bounds are smaller for the Jansen than the Sobol estimators. For the Sobol estimators the confidence intervals are overlapping such that a clear differentiation of the effects is not possible.

Based on these convergence results, as outlined in Figure 6 and 7, in the following analyses only the results of the Jansen estimators are further considered.

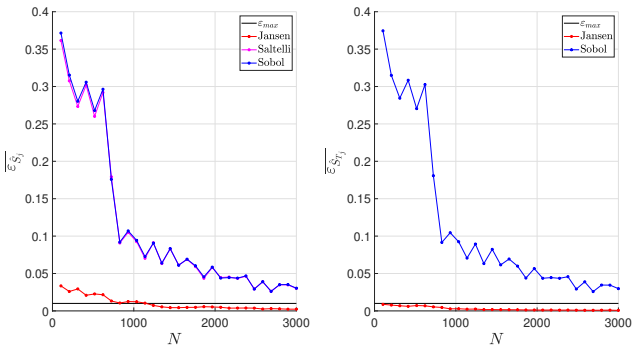

Fig. 6. Convergence errors $\overline{\varepsilon_{\hat{S}_j}}$ and $\overline{\varepsilon_{\hat{S}_{T_j}}}$ for all estimators and a defined maximum error bound ε_{max}.

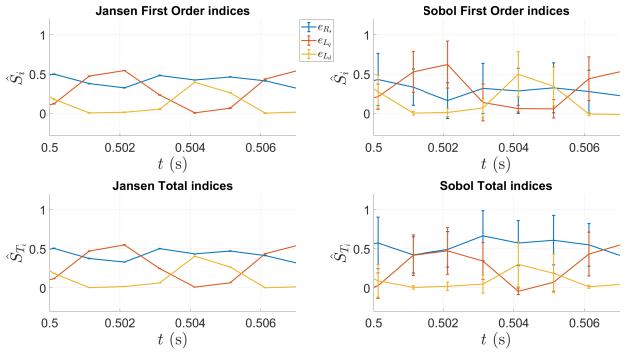

Fig. 7. 95% confidence intervals of Jansen (1999) and Sobol (1993),Sobol (2007) estimators for $\hat{S}_i$ and $\hat{S}_{T_i}$ at the time interval $[0.5\,\text{s}, 0.508\,\text{s}]$

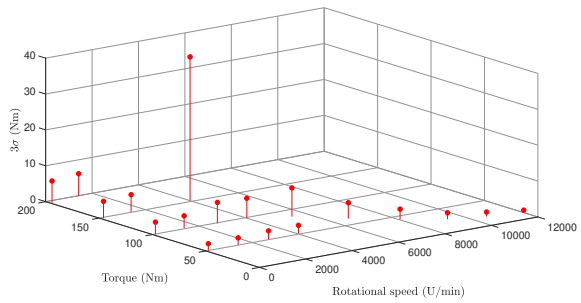

Fig. 8. 3σ bounds for the simulated operating points

5.2 Sensitivity analysis of the torque accuracy

In the first step the maximum absolute deviation is analyzed. The 3σ bound of the variance is defined as measure of the variation in the output torque and is depicted in Figure 8. In general, the maximum deviation of the torque is less than 10 Nm except for one single working point. The absolute fluctuation should always be taken into account to identify the working points with the highest deviation.

In order to quantify the influence of each parameter at each operating point the computed sensitivity indices for 19 working points are used. They are outlined in Figure 9 for the first order effects and in Figure 10 for the total effects. Comparing the first order and the total order effects in the continuous torque area, it can be seen that the parameter dependencies behave linear since $\sum_{i=1}^{K} \hat{S}_i \approx$

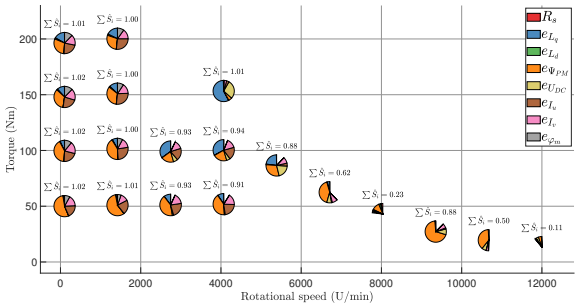

Fig. 9. First order effects for different operating points

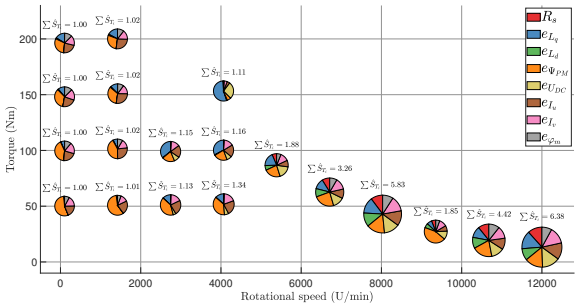

Fig. 10. Total order effects for different operating points

$\sum_{i=1}^{K} \hat{S}_{T_i}$ holds. This means that the effect $\hat{S}_{T_i}$ on the output variance depends only on one parameter and has no interaction with other parameters. On the other hand in the field weakening area and at the power boundary the system behaves nonlinear or with interactions with other parameters because of $\sum_{i=1}^{K} \hat{S}_i \neq \sum_{i=1}^{K} \hat{S}_{T_i}$ or $\sum_{i=1}^{K} \hat{S}_{T_i} \gg 1$.

The first order indices show that for almost each working point the variation in the magnetic flux $e_{\Psi_{PM}}$ has a significant influence on the torque accuracy. Also the current errors e_{I_u} and e_{I_v} are responsible for a large share of variance of the torque but mainly in the continuous torque area. In the field weakening area a lot of nonlinear effects exist, because of $\sum_{i=1}^{K} \hat{S}_i \ll 1$. Nevertheless, Figure 10 outlines that in the field weakening area each parameter has nearly the same influence on the variance of the torque. Therefore, in this case no dominant parameter such as in the continuous torque area can be figured out.

Based on these results, it is outlined that the torque accuracy can be systematically improved for the continuous torque area by focusing on the significant parameters $e_{\Psi_{PM}}$,e_{I_u} and e_{I_v}. Unfortunately, in the examined system no significant parameter for the field weakling area can be established. Nevertheless, with this knowledge developers are able to focus on the relevant parts of the system for improvements and to save time and money.

6. CONCLUSION

This paper outlines the benefits of a variance based sensitivity analyses on a real physical system. A complete BEV powertrain was modeled and used as the basis for the sensitivity analysis. To deal with the problem of ensuring convergence two novel approaches were discussed. Moreover, the link between the variance based sensitivity measures and the application on physical models, including time and state dependence, was derived. Finally, the convergence error and the sensitivity indices were computed and discussed for the presented system.

The results indicate that the variance based sensitivity analysis is a powerful method to connect the effects on the output with their causes. This makes it possible to quantify the influence of dominant parameters on the torque accuracy in electrical drives. As a result, the developer is able to identify the most influencing parameters to reduce the torque deviation with minimal effort in cost and time.

REFERENCES

Archer, G.E.B., Saltelli, A., and Sobol, I.M. (1997). Sensitivity measures, anova-like techniques and the use of bootstrap. *Journal of Statistical Computation and Simulation*, 58(2), 99–120. doi:10.1080/00949659708811825.

Efron, B. (1979). Bootstrap methods: Another look at the jackknife. *The Annals of Statistics*, 7(1), 1–26.

Jansen, M.J. (1999). Analysis of variance designs for model output. *Computer Physics Communications*, 117(1-2), 35–43. doi:10.1016/S0010-4655(98)00154-4.

Menberg, K., Heo, Y., and Choudhary, R. (2016). Sensitivity analysis methods for building energy models: Comparing computational costs and extractable information. *Energy and Buildings*, 133, 433–445. doi:10.1016/j.enbuild.2016.10.005.

Opalski, L.J. (2015). Efficient global sensitivity analysis method for models of systems with functional outputs. In *2015 European Conference on Circuit Theory and Design (ECCTD)*, 1–4. IEEE. doi:10.1109/ECCTD.2015.7300048.

Saltelli, A., Annoni, P., Azzini, I., Campolongo, F., Ratto, M., and Tarantola, S. (2010). Variance based sensitivity analysis of model output. design and estimator for the total sensitivity index. *Computer Physics Communications*, 181(2), 259–270. doi:10.1016/j.cpc.2009.09.018.

Schröder, D. (2013). *Elektrische Antriebe - Grundlagen*. Springer-Lehrbuch. Springer Berlin Heidelberg, Berlin, Heidelberg, 5 edition. doi:10.1007/978-3-642-30471-2.

Schwieger, V. (2007). Sensitivity analysis as a general tool for model optimisation – examples for trajectory estimation. *Journal of Applied Geodesy*, 1(1), 27–34. doi:10.1515/jag.2007.004.

Sobol, I.M. and Kucherenko, S.S. (2005). On global sensitivity analysis of quasi-monte carlo algorithms. *Monte Carlo Methods and Applications*, 11(1), 83–92. doi:10.1515/1569396054027274.

Sobol, I.M. (1967). On the distribution of points in a cube and the approximate evaluation of integrals. *USSR Computational Mathematics and Mathematical Physics*, 7(4), 784–802. doi:10.1016/0041-5553(67)90144-9.

Sobol, I.M. (1993). Sensitivity analysis for nonlinear mathematical models. *Mathematical Modeling and Computational Experiments*, 1(4), 407–414.

Sobol, I.M. (2007). Global sensitivity indices for the investigation of nonlinear mathematical models. *Matematicheskoe Modelirovanie*, 19(11), 23–24.